Synthetic Dioxygen-carrying Hemoprotein. Human Serum Albumin Including Iron(II) Complex of Protoporphyrin IX with an Axially Coordinated Histidylglycyl-propionate

Akito Nakagawa, Teruyuki Komatsu, Naomi Ohmichi, and Eishun Tsuchida*
Advanced Research Institute for Science and Engineering, Waseda University, 3-4-1 Okubo Shinjuku-ku, Tokyo 169-8555

(Received February 28, 2003; CL-030171)

Human serum albumin incorporating the iron(II) complex of protoporphyrin IX having an axially coordinated histidylglycyl-propionate formed a dioxygen-adduct complex in aqueous media (pH 7.3). The O_2-binding affinity ($P_{1/2}$) was 0.1 Torr at 25 °C.

Apomyoglobin spontaneously incorporates an iron(III) complex of protoporphyrin IX (hemin) and enable the prosthetic group to bind a dioxygen molecule (O_2).[1,2] Human serum albumin (HSA), the most abundant plasma protein in our blood stream, also captures a hemin dissociated from methemoglobin and accommodates it in the subdomain IB.[3,4] However, this HSA-hemin hybrid cannot form the O_2-adduct complex, even if one reduces the central ferric ion of the hemin to the ferrous state. We have shown that HSA including highly encumbered tetraphenylporphinato-iron(II) (Fe^{2+}TPP) derivatives can only bind and release O_2 under physiological conditions similar to hemoglobin (Hb) and myoglobin (Mb).[5] The prerequisites of these stable dioxygenations were believed to provide the Fe^{2+}TPP structure with (i) steric hindrance around the O_2-binding site to prevent proton access, and (ii) a covalently bound proximal imidazole. More recently, we have found that the iron(II) complex of protoporphyrin IX having an axially coordinated histidylglycyl-propionate is also included into the HSA interior and forms an O_2-adduct in aqueous media at 25 °C. This communication reports for the first time the HSA hybrids incorporating natural protoheme IX derivatives as novel synthetic O_2-carrying hemoproteins.

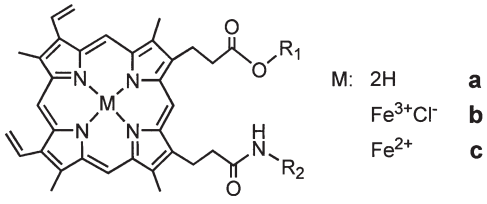

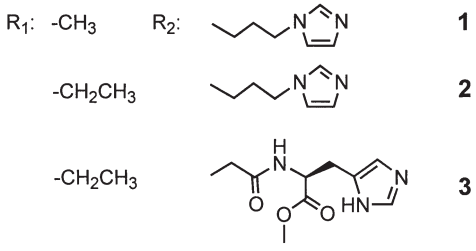

The free-base porphyrin of the pioneering Mb model, chelated heme **1a**,[6] was synthesized by our one-pot reaction procedure using benzotriazol-1-yloxytris(dimethylamino)phosphonium hexafluorophosphate (BOP) at room temperature in pyridine. After the reaction, the mixture, when poured into excess water, led to precipitation of the crude product; the pyridine, water soluble BOP, and formed hexamethylphosphoramide were easily filtered off. Compound **2a** with an ethyl propionate, and compound **3a** having a histidylglycyl-propionate were also prepared in the same manner (Yield: 30%).[7] The iron insertion was performed using $FeCl_2$ in DMF to give the corresponding hemin derivatives. The analytical data of all compounds were satisfactorily obtained.[8]

The UV–vis absorption spectrum of the ferrous complex **3c** (λ_{max}: 423, 533, 555 nm) in DMF showed the formation of the typical five-*N*-coordinated high-spin iron(II) complex as well as **1c** and **2c**. Upon the bubbling of O_2 gas through this solution, the UV–vis absorption immediately changed to that of the O_2-adduct complex (λ_{max}: 408, 540, 575 nm). The dioxygenated **3c** transferred to the stable carbonyl species (λ_{max}: 419, 537, 568 nm) after the exposure of carbon monoxide (CO). The O_2-binding affinity ($P_{1/2}$) of **3c** was determined to be 0.2 Torr in DMF solution, which is slightly lower (high affinity) than those of **1c** and **2c** ($P_{1/2}$: 0.3 Torr) (Table 1).[6d] The O_2-binding affinity normally elevates in proportion to an increase in the basicity of the trans-coordinated imidazole,[9] but histidine in **3c** showed a smaller pK_a (6.0) in comparison to the value of 1-(acetoamidopropyl)imidazole (pK_a = 6.6) for **2c**. The high O_2-binding affinity of **3c** is presumably due to a favorable geometry of the imidazole bonding to the central iron, which was supported by the preliminary results on our molecular simulations of the dioxygenated **3c** complex.[10]

The hybridization of HSA and the protoheme IX derivatives (molar ratio: 1/1) were carried out as follows. The ethanol solution of the carbonylated heme (1.6 mM, 50 μL) was slowly injected into the phosphate buffered solution (pH 7.3, 1 mM) of the recombinant HSA (rHSA)[11] (20 μM, 4 mL) under an argon atmosphere. The obtained aqueous solutions were stable for a few months without precipitation. The UV–vis absorption spectra of the rHSA-heme hybrids showed formation of the CO-ad-

Table 1. O_2-binding parameters of rHSA-protoheme IX derivatives at 25 °C

	pK_a	$P_{1/2}$ (Torr)		$\tau_{1/2}$ (min)
		in DMF	rHSA hybrid in water	rHSA hybrid in water
1c	6.6[a]	0.3	0.1	20
		0.3[b]	1.0[c]	—
2c	6.6[a]	0.3	0.1	50
3c	6.0[d]	0.2	0.1	90

[a]p*Ka* value of 1-(acetoamidoprpoyl)imidazole in water (Ref. 6b), [b]Ref. 6d, [c]2% Aqueous myristyltrimethylammonium-bromide suspension (Ref. 6c). [d]p*Ka* value of histidine in water.

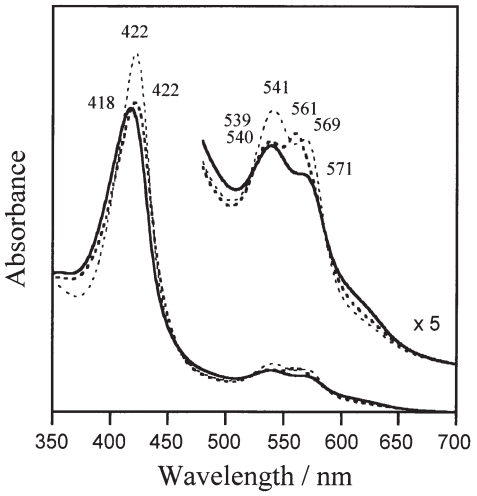

Figure 1. UV–vis absorption spectral changes of rHSA-**3c** in phosphate buffered solution (pH 7.3, 25 °C); under Ar: - - - -, under O_2: —, under CO: · · · · · · ·.

duct complexes (Figure 1). The binding number of protoheme IX derivative in one albumin molecule was confirmed to be one by assay of the each concentration and the relatively high binding constants of the hemes for rHSA (K_1: ca. $4 \times 10^6\ M^{-1}$). The isoelectric points ($pI = 4.8$) and circular dichloism spectra of rHSA-hemes were identical to those observed for rHSA itself, which indicated that the surface net charges and second-order structure of rHSA host did not change after incorporation of the heme guest. Light irradiation of the carbonyl complex of rHSA–**3c** led to CO dissociation and a changing of spectrum, in which two peaks appeared in the Q band region; the resulting spectral shape resembles that of the six-coordinated low-spin mesoheme derivatives.[6b] This result implies that the sixth coordination site of **3c** is occupied by some amino acid residue of albumin. The spectral feature of rHSA–**1c** and rHSA–**2c** also showed the same trend.

Upon exposure of the rHSA–**3c** solution to O_2, the UV–vis absorption spectrum rapidly changed to that of the O_2-adduct complex (Figure 1). From the recent result on our crystal structural analysis of rHSA-hemin hybrid,[4] we infer that the protoheme derivatives **1c**, **2c**, and **3c** are also accommodated into the hydrophobic site of the subdomain IB, and it may contribute to their O_2-adduct complex formation. The O_2-binding affinity ($P_{1/2}$) of rHSA–**2c** and rHSA–**3c** were determined to be both 0.1 Torr. Accompanying the autooxidation of the central iron(II), the absorption band (λ_{max}: 540, 571 nm) slowly decreased, leading to the formation of the inactive protohemin. The half life-times ($\tau_{1/2}$) of the O_2-adduct species for rHSA–**2c** and rHSA–**3c** were 50 min and 90 min, respectively (Table 1). We concluded that the axially bound histydylglycyl-propionate to protoheme IX provided a more stable O_2-adduct compared to the imidazolyl one, and the ethyl propionate on the other side also contributed the increased stability for the dioxygenated complex relative to the methyl-propionate ($\tau_{1/2}$ of rHSA–**1c**: 20 min).

In conclusion, rHSA successfully incorporated protoheme IX derivatives with an intramolecularly coordinated proximal base, giving rHSA-heme hybrids, which form O_2 adducts at 25 °C. These are the first examples of the synthetic O_2-carrying hemoproteins containing the natural protoheme IX derivative as a prosthetic group, which may also act as a very new class of artificial hemoprotein enzymes as well.

This work was partially supported by Health Science Research Grants (Research on Pharmaceutical and Medical Safety) of the MHLW, and by a Grant-in-Aid for Scientific Research (No. 13650938) from the MEXT.

References and Notes

1 T. Hayashi, H. Dejima, T. Matsuo, H. Sano, D. Murata, and Y. Hisaeda, *J. Am. Chem. Soc.*, **124**, 11226 (2002).
2 S. Neya, K. Imai, H. Hori, H. Ishikawa, K. Ishimori, D. Okuno, S. Nakatomo, T. Hoshino, M. Hata, and N. Funasaki, *Inorg. Chem.*, **42**, 1456 (2003).
3 M. Wardell, Z. Wang, J. X. Ho, J. Robert, F. Ruker, J. Ruble, and D. C. Carter, *Biochem. Biophys. Res. Commun.*, **291**, 813 (2002).
4 P. A. Zunszain, J. Ghuman, T. Komatsu, E. Tsuchida, and S. Curry, "Protein Data Bank," code: 1O9X, paper in preparation.
5 a) T. Komatsu, K. Ando, N. Kawai, H. Nishide, and E. Tsuchida, *Chem. Lett.*, **1995**, 813. b) T. Komatsu, K. Hamamatsu, J. Wu, and E. Tsuchida, *Bioconjugate Chem.*, **10**, 82 (1999). c) E. Tsuchida, T. Komatsu, Y. Matsukawa, K. Hamamatsu, and J. Wu, *Bioconjugate Chem.*, **10**, 797 (1999). d) T. Komatsu, T. Okada, M. Moritake, and E. Tsuchida, *Bull. Chem. Soc. Jpn.*, **74**, 1695 (2001). e) T. Komatsu, Y. Matsukawa, and E. Tsuchida, *Bioconjugate Chem.*, **13**, 397 (2002).
6 a) W. S. Brinigar, C. K. Chang, J. Geibel, and T. G. Traylor, *J. Am. Chem. Soc.*, **96**, 5597 (1974). b) J. Geibel, J. Cannon, D. Chambell, and T. G. Traylor, *J. Am. Chem. Soc.*, **100**, 3575 (1978). c) T. G. Traylor, C. K. Chang, J. Geibel, A. Berzinis, T. Mincey, and J. Cannon, *J. Am. Chem. Soc.*, **101**, 6716 (1979). d) T. G. Traylor and P. S. Traulor, *Annu. Rev. Biophys. Bioeng.*, **11**, 105 (1982).
7 Glycyl-L-histidine methyl ester dihydrochloride was prepared according to the previously reported procedures [E. Monzani, L. Linati, L. Casella, L. D. Gioia, M. Favretto, M. Gullotti, and F. Chillemi, *Inorg. Chim. Acta*, **273**, 339 (1998)].
8 Spectoscopic data: **2a**; ^{1}H-NMR (500 MHz, $CDCl_3$) δ −3.6 (s, 2H, inner-H), 0.9 (t, -COO-CH_2CH_3, 3H), 1.1–1.5 (m, 2H, -CH_2CH_2-imidazole (Im)), 2.9–3.1 (m, -C(=O)NH-CH_2CH_2-, 2H), 3.1–3.3 (m, -CH_2CH_2COO-, 4H), 3.4–3.7 (m, porphyrin (por.)-CH_3, -CH_2CH_2-Im, 14H), 3.7–3.9 (m, -COO-CH_2CH_3, 2H), 4.1–4.4 (m, por.-CH_2-, 4H), 5.9–6.4 (m, vinyl =CH_2, Im, 5H), 6.6 (d, Im , 1H), 6.9 (s, Im , 1H), 8.1–8.3 (m, vinyl-C*H*=, 2H), 9.8–10.1 (m, *meso*, 4H), FAB-MS (*m*/*z*): 698.4 [M-H$^+$]. IR (cm^{-1}): 1650 ($\nu_{C=O}$ (amido)), 1732 ($\nu_{C=O}$ (ester)). UV–vis ($CHCl_3$) λ_{max}: 409, 509, 544, 580, 633 nm. **2b**; FAB-MS (*m*/*z*): 752.4 [M-Cl$^-$]. IR (cm^{-1}): 1651 ($\nu_{C=O}$ (amido)), 1725 ($\nu_{C=O}$ (ester)). UV–vis ($CHCl_3$) λ_{max}: 406, 520, 578 nm. **3a**; ^{1}H-NMR (500 MHz, $CDCl_3$) δ −4.6 (s, 2H, inner-H), 2.7–2.9 (m, Im-CH_2-, 2H), 3.0–3.5 (m, por.-CH_3, -CH_2CH_2CONH-, -CH_2 CH_2-COO-CH_2CH_3, 18H), 3.6 (s, -CONH-CH_2CONH-, 2H), 4.0–4.3 (d, por.-CH_2, 4H), 4.3–4.5 (m, α-C*H*, 1H), 6.0–6.4 (m, vinyl =CH_2, 4H), 7.4 (s, Im , 1H), 8.0–8.3 (m, vinyl-C*H*=, Im, 5H), 9.8–10.0 (m, *meso*, 4H), FAB-MS (*m*/*z*): 785.4 [M-H$^+$]. IR (cm^{-1}): 1635 ($\nu_{C=O}$ (amido)), 1725 ($\nu_{C=O}$ (ester)). UV–vis ($CHCl_3$) λ_{max}: 405, 505, 541, 577, 627 nm. **3b**; FAB-MS (*m*/*z*): 838.4 [M-Cl$^-$]. IR(cm^{-1}): 1660 ($\nu_{C=O}$ (amido)), 1734 ($\nu_{C=O}$ (ester)). UV–vis ($CHCl_3$) λ_{max}: 388, 508, 637 nm.
9 D. V. Stynes, H. C. Stynes, B. R. James, and J. A. Ibers, *J. Am. Chem. Soc.*, **95**, 1796 (1973).
10 The esff forcefield simulation was performed using an Insight II system (Molecular Simulation Inc.). The structure was generated by alternative minimization and annealing dynamic calculation.
11 A. Sumi, W. Ohtani, K. Kobayashi, T. Ohmura, K. Tokoyama, M. Nishida, and T. Suyama, "Biotechnology of Blood Proteins," John Libbey Eurotext, Montrouge (1993), Vol. 227, p 293.

Published on the web (Advance View) May 13, 2003; DOI 10.1246/cl.2003.504